

A nuclear-targeted effector of *Rhizophagus irregularis* interferes with histone 2B mono-ubiquitination to promote arbuscular mycorrhisation

Peng Wang¹ , Henan Jiang¹, Sijf Boeren², Harm Dings¹, Olga Kulikova¹, Ton Bisseling¹  and Erik Limpens¹ 

¹Laboratory of Molecular Biology, Wageningen University & Research, Wageningen 6708 PB, the Netherlands; ²Laboratory of Biochemistry, Wageningen University & Research, Wageningen 6708 WE, the Netherlands

Author for correspondence:

Erik Limpens

Email: erik.limpens@wur.nl

Received: 4 September 2020

Accepted: 18 January 2021

New Phytologist (2021)

doi: 10.1111/nph.17236

Key words: arbuscular mycorrhiza (AM), effector, H2B mono-ubiquitination, plant defence, *Rhizophagus irregularis*, symbiosis.

Summary

- Arguably, symbiotic arbuscular mycorrhizal (AM) fungi have the broadest host range of all fungi, being able to intracellularly colonise root cells in the vast majority of all land plants. This raises the question how AM fungi effectively deal with the immune systems of such a widely diverse range of plants.
- Here, we studied the role of a nuclear-localisation signal-containing effector from *Rhizophagus irregularis*, called Nuclear Localised Effector1 (RiNLE1), that is highly and specifically expressed in arbuscules.
- We showed that RiNLE1 is able to translocate to the host nucleus where it interacts with the plant core nucleosome protein histone 2B (H2B). RiNLE1 is able to impair the mono-ubiquitination of H2B, which results in the suppression of defence-related gene expression and enhanced colonisation levels.
- This study highlights a novel mechanism by which AM fungi can effectively control plant epigenetic modifications through direct interaction with a core nucleosome component. Homologues of RiNLE1 are found in a range of fungi that establish intimate interactions with plants, suggesting that this type of effector may be more widely recruited to manipulate host defence responses.

Introduction

Microbes that intimately interact with plants face the challenge of dealing with the plant's immune system. Conserved microbe-associated molecular patterns (MAMPs) such as chitin or beta-glucans present in the cell walls of such microbes are potent triggers of defence responses in the plant. Pathogens typically subvert host immunity by secreting a range of effector proteins that can act outside or inside the host cell (Lo Presti *et al.*, 2015). Recent studies on several pathogenic effector proteins that are translocated into plant cells have revealed that epigenetic modifications are a key target to suppress immunity genes (Ramirez-Prado *et al.*, 2018). Transcriptional reprogramming plays a central role in plant immunity (Jenner & Young, 2005). In particular, various histone modifying enzymes have been found to be a target of oomycete or fungal effector proteins to suppress defence gene expression. For example, the *Phytophthora sojae* effectors Avr52 and PsAvh23 and the nonribosomal HC Toxin peptide from the maize pathogen *Cochliobolus carbonum* were shown to target histone acetyltransferases to modify histone acetylation levels, causing the suppression of defence gene expression or the activation

of susceptibility genes (Ransom & Walton, 1997; Walley *et al.*, 2008; Kong *et al.*, 2017; Li *et al.*, 2018).

Similar to fungal pathogens, also mutualistic arbuscular mycorrhizal (AM) fungi, belonging to the Glomeromycotina subphylum, contain chitin and beta-glucans in their cell walls (Lo Presti *et al.*, 2015; Wawra *et al.*, 2016; Zeng *et al.*, 2020). AM fungi form root symbiotic associations with the vast majority (>75%) of land plant species (Smith & Read, 2008). In this intimate partnership, the biotrophic AMF form highly branched arbuscules inside root cortex cells, where they provide the plant host with mineral nutrients such as phosphate and ammonium, in return for plant-derived photosynthates (Gutjahr & Parniske, 2013). The apparent lack of host specificity in this interaction indicates that AM fungi must have broadly effective mechanisms to subvert the host immune system in such a wide variety of plants (Volpin *et al.*, 1994; García-Garrido & Ocampo, 2002). In comparison, most pathogenic fungi typically have a rather narrow host range. Like their pathogenic counterparts, AM fungi also make use of effector proteins to deal with the plant immune system (Kloppholz *et al.*, 2011; Zeng *et al.*, 2020). However, the various mechanisms by which AM fungal effector proteins

manipulate plant responses and contribute to their broad host range are far from understood (Tisserant *et al.*, 2013; Lin *et al.*, 2014; Kamel *et al.*, 2017; Voß *et al.*, 2018; Zeng *et al.*, 2018).

In previous work we showed that many putative effector proteins from *Rhizophagus irregularis* are expressed at distinct stages of the interaction (Zeng *et al.*, 2018). Several effector candidates were shown to be specifically expressed in arbuscules when the fungus intracellularly colonised root cortex cells. One of the highest expressed putative effectors in arbuscules encoded a small secreted protein containing a nuclear-localisation signal. Here we show that this effector, which we called NUCLEAR LOCALIZING EFFECTOR 1 (RiNLE1), can translocate to the host nucleus where it interacts with the core nucleosome protein histone 2B. RiNLE1 impairs the mono-ubiquitination of H2B, resulting in reduced expression of a set of defence-related genes and enhanced mycorrhizal colonisation levels. This reveals that epigenetic reprogramming is a common target of pathogenic and mutualistic fungal effectors and identifies the direct targeting of H2B as a novel mechanism for fungal effector proteins.

Materials and Methods

Plant and fungal material

Medicago truncatula Jemalong A17 (Medicago) seedlings were grown and transformed as described previously (Limpens *et al.*, 2004). *Nicotiana benthamiana* was used for *Agrobacterium tumefaciens*-mediated transient expression as described before (Zeng *et al.*, 2018). *Rhizophagus irregularis* DAOM197198 spores were obtained from Agronutrition, France. Spores were washed thoroughly through three layers of filter mesh (220, 120, 38 µm) before use. Plants for mycorrhisation were grown in SC10 RayLeach cone-tainers (Stuewe and Sons, Canada) containing a premixed sand : clay (1 : 1, v/v) mixture and inoculated by placing *c.* 200 pores *c.* 2 cm below the seedling roots. Plants were grown in a 16 h daylight chamber at 21°C and watered with 10 ml half-strength Hoagland medium with 20 µM phosphate twice a week (Zeng *et al.*, 2018).

Cloning

Unless indicated, all the constructs used in this work were made using the Golden Gate cloning system (Engler *et al.*, 2014). All primers used are listed in Supporting Information Table S1. The vectors used for cloning of the different constructs are listed in Table S2. All newly made level zero cloning vectors were confirmed by sequencing.

Phylogeny

For phylogenetic analyses, RiNLE1 homologues were collected using the protein–protein BLAST algorithm from NCBI and JGI. To select the effector homologues, the following criteria were used: (1) protein should be predicted to have a signal peptide using the SIGNALP-5.0 server (<http://www.cbs.dtu.dk/services/SignalP/>); (2) the proteins should be predicted to be a potential

effector based on EFFECTORP 2.0 software (<http://effectorp.csiro.au/>); (3) the proteins should be predicted to be nuclear localised based on LOCALIZER software (<http://localizer.csiro.au/>). Identified homologues were aligned using the MAFFT program built in GENEIOUS R11.0 software (<https://www.geneious.com>). An unrooted phylogenetic tree was generated using the neighbour-joining tree builder in GENEIOUS R11.0.

RNA *in situ* hybridisation

Medicago roots hosting the AM fungus were fixed with 4% paraformaldehyde mixed with 3% glutaraldehyde in 50 mM phosphate buffer (pH 7.4) overnight, dehydrated in serial dilution of ethanol and then embedded in paraffin (Paraplast X-tra; McCormick Scientific, St Louis, MO, USA) as described (Kulikova *et al.*, 2018). Next, 7-µm-thick root sections were cut using an RJ2035 microtome (Leica). RNA *in situ* hybridisation was conducted using Invitrogen ViewRNA ISH Tissue 1-Plex Assay kits (Thermo Fisher Scientific, Waltham, MA, USA) according to the user manual available online (short-url.at/fuzPT).

RNA ISH probe sets were designed and synthesised by request at Thermo Fisher Scientific. A typical probe set consisted of *c.* 20 synthetic adjacent oligonucleotide pairs. Each of these pairs was composed of a 20-bp primary sequence designed to target specific regions across the target mRNA sequence and a secondary extended sequence serving as a template for the amplification and detection of hybridisation signals. A probe set for *RiNLE1* (catalogue number VF1-6001202) covered the mRNA sequence from 2 bp to 613 bp and a probe set for *MtPT4* (VF1-19337) covered the region from 390 bp to 1296 bp. A probe set for *MtPT4* was used as a positive control for *in situ* hybridisation. As a negative control, a *RiNLE1* sense probe set (VPEPR3M) was used and probe sets were omitted for hybridisation.

Localisation of RiNLE1

To check the subcellular localisation of RiNLE1, a PT4p::GFP-RiNLE1 (lacking the endogenous signal peptide) construct was transformed into Medicago using *Agrobacterium rhizogenes* MSU440-mediated hairy root transformation (Limpens *et al.*, 2004). At 5 wk after inoculation with 200 *R. irregularis* spores, transgenic mycorrhizal roots were harvested for confocal microscopy to check the localisation of RiNLE1.

Yeast secretion trap

The yeast signal sequence trap (YSST) method was carried out using *Saccharomyces cerevisiae* Y02321 strain (Euroscarf, Frankfurt, Germany), and following a protocol described previously (Zeng *et al.*, 2020). Briefly, the *RiNLE1* full coding sequence without the stop codon was inserted into the *EcoRI* and *NotI* sites of the pYST0 plasmid (Lee *et al.*, 2006). Positive colonies from SD/-LEU plates were plated on sucrose selection medium (2% sucrose, 0.025% glucose, 6.7 g l⁻¹ yeast nitrogen base without amino acids, 1.85 g l⁻¹ Drop-out mix minus leucine, 2% agar)

and incubated at 30°C for 3–5 d. The pYST0 empty vector transformed Y02321 strain was used as a control.

Agroinfiltration of *Nicotiana benthamiana*

To determine whether the RiNLE1 protein can cross the plant cell wall and enter the nucleus, a UBp::BCP1sp-GFP-RiNLE1 construct was transiently expressed in *Nicotiana benthamiana* (Nicotiana) leaves. UBp::BCP1sp-GFP was used as a control. *Agrobacterium* infiltration of 5-wk-old Nicotiana leaves was performed as described before (Zeng *et al.*, 2018), using co-transformed P19 as the silencing inhibitor. The infiltrated plants were grown for 2 d and samples were collected for confocal microscopy using a Leica SP8 confocal microscope.

Hypersensitive response

The effect of RiNLE1 on the AVR4- and CF-4 induced hypersensitive response (HR) was carried out as described (Ma *et al.*, 2012). *Nicotiana benthamiana* leaves were infiltrated with different combination of *Agrobacterium* carrying constructs and grown for 4 d in a glasshouse, after which the leaves were harvested for trypan blue staining. The leaves were boiled in 50 ml staining solution (10 ml lactic acid, 10 ml phenol, 10 ml glycerol, 10 ml H₂O and 10 mg trypan blue) mixed with 50 ml 96% ethanol for 5 min. Subsequently, the leaves were destained (250 g chloral hydrate in 100 ml H₂O) overnight at room temperature.

Co-immunoprecipitation (Co-IP) and liquid chromatography tandem-mass spectrometry (LC-MS/MS)

For identification of RiNLE1 interactors, a PT4p::FLAG-RiNLE1 construct was transformed into *Medicago* roots as described before. PT4p::FLAG-GFP transformed roots were used as a negative control. Total proteins were extracted from well mycorrhised transgenic roots using Co-IP buffer (10% glycerol, 50 mM Tris-HCl pH 8.0, 150 mM NaCl, 1% Igepal CA 630, 1 mM PMSF, 20 µM MG132, one tablet protease inhibitor cocktail). The total protein mix was centrifuged at 18 580 g for 10 min at 4°C, and then the supernatant was transferred to a fresh 15 ml tube. Next, the sample was centrifuge at maximum speed for 10 min at 4°C, and the supernatant transferred to a new 15 ml tube; the FLAG-tagged protein was pulled down using µMACS and MultiMACS DYKDDDDK Isolation Kits (Miltenyi Biotec). Immunoprecipitated protein samples were digested into peptides using trypsin (Sigma-Aldrich).

Peptide samples were measured using nLC-MS/MS with a Proxeon EASY nLC1000 and a LTQ-Orbitrap XL mass spectrometer as previously described (Lu *et al.*, 2011; Wendrich *et al.*, 2017). Briefly, 18 µl of peptide sample was injected over a 0.10 × 32 mm Magic C18AQ 200A 5-µm bead (Bruker Nederland BV, Leiderdorp, the Netherlands) preconcentration column (prepared in house) and peptides were eluted onto a 0.10 × 250 mm ReproSil-Pur 120 C18-AQ 1.9 µm bead analytical column (prepared in house) with an acetonitrile gradient at a flow rate of 0.5 µl min⁻¹ using a Thermo Scientific EASY-nLC

1000 liquid chromatography system. A gradient from 9 to 34% acetonitrile in water with 1 ml l⁻¹ formic acid was applied in 50 min. An electrospray potential of 3.5 kV was applied directly to the eluent and full scan positive mode Fourier transform mass spectrometry (FTMS) spectra were measured between *m/z* 380 and 1400 in an Orbitrap[®] mass spectrometer at high resolution (60 000) and MS/MS spectra were measured in the ion trap.

LC-MS data analysis (false discovery rates were set to 0.01 on peptide and protein levels) and additional result filtering (minimally two peptides are necessary for protein identification of which at least one is unique and at least one is unmodified) were performed as described previously (Smaczniak *et al.*, 2012; Wendrich *et al.*, 2017). Peptide data were mapped to *Medicago truncatula* UniProt 2018 and *Rhizophagus irregularis* DAOM197198 UniProt 2018 to identify proteins. To analyse the relative abundance of proteins, their normalised label-free quantification (LFQ) intensities were compared (Cox *et al.*, 2014). nLC-MSMS system quality was checked with Proteomics Quality Control (PTXQC) (Bielow *et al.*, 2016) using the MAXQUANT result files.

Yeast-two-hybrid assay

To confirm interactions, yeast-two-hybrid analyses were applied using the Matchmaker Gold Yeast-Two-Hybrid System (Clontech, USA) according to manufacturer's instructions. *RiNLE1* was inserted into the pGBKT7 bait vector, *MtH2B.1* was inserted into the pGADT7 prey vector. Bait and prey constructs were transformed into Y2H Gold and Y187 strains as described in instruction for the Matchmaker system, respectively. Bait and prey strains were mated following the manufacturer's handbook (Clontech, USA). After mating, yeast was plated on DDO and QDO/X/A plates to check mating and protein–protein interaction results, respectively.

Dexamethasone inducible RiNLE1 expression

The dexamethasone (DEX) inducible expression system (Borghi, 2010) was applied to induce *RiNLE1* expression in *Medicago* hairy roots. First, construct LjUB1::GVG–AtUB10::DsRed–UAS::RiNLE1–UAS::GFP and control construct LjUB1::GVG–AtUB10::DsRed–Dummy3 (GCAACATACGCTGGA)–UAS::GFP were transformed into *Medicago* hairy roots as described previously (Limpens *et al.*, 2004). Composite plants containing transgenic roots were transferred to Emergence medium plates (Limpens *et al.*, 2004). Three plants were collected for one repetition. After 1 d, 2 ml of 10 µM DEX dissolved in DMSO were spread onto the roots by pipetting. After 20 h, a clear GFP signal was visible under a fluorescence microscope. Transgenic roots were harvested and stored in –80°C for further analysis.

RNA isolation and qPCR

All RNA samples in this work were isolated using the Qiagen plant RNA mini kit, following the manufacturer's instructions. cDNA was made from 200 ng RNA using the iScript cDNA Synthesis kit (Bio-Rad). iQ SYBR Green Supermix (Bio-Rad) was

chosen for qPCR using the Bio-Rad CFX connect real-time system. Primers used are listed in Table S1. Gene expression was normalised using *Medicago* Elongation factor 1 (*EF1*). Relative expression levels were calculated as $2^{-\Delta\Delta C_t}$. Three technical replicates were used for each sample.

RNA sequencing

RNA was isolated as described above. Three transformed plants grown on one Emergence plate was used as one replicate. Three replicates were used for RNA-seq. RNA samples were sequenced using the BGI SEQ-500 Transcriptome platform. RNA-seq data were mapped to the *Medicago truncatula* genome v4.0 using a CLC Genomics workbench 10.0.1 (Qiagen). Settings for transcripts per million (TPM), principal component analysis (PCA) and differential expression analyses were performed as described by Zeng *et al.* (2018). RNA-seq data were deposited to the NCBI Gene Expression Omnibus, under the accession number GSE155682.

RiNLE1 constitutive overexpression

For constitutive *RiNLE1* overexpression, RiNLE1 was expressed in *Medicago* hairy roots under the control of the *Lotus Ubiquitin 1* promoter. An empty vector construct was used as the control. Transgenic roots were harvested 3 wk after inoculation for mycorrhizal quantification and RNA isolation. Roots for mycorrhizal quantification were stained with WGA-Alexafluor 488 (Thermo Fisher Scientific) and scored using the gridline intersect method (McGonigle *et al.*, 1990).

Host-induced gene silencing

RiNLE1 hairpin constructs were generated using the Gateway system (Invitrogen, USA). RiNLE1 mRNA sequences were amplified and cloned into the pENTR/D-TOPO entry vector. Primers used are listed in Table S1. Next, a fragment of RiNLE1 was cloned into the modified pK7GWIG2(II)-AtEF1 RR vector using LR clonase II (Invitrogen) to produce the final silencing construct. An empty vector was used as the control. *Medicago* A17 transformation, spore inoculation and mycorrhizal quantification were carried out as described previously.

HUB1 experiments

The *Medicago HUB1* CDS (Medtr7g046250) was amplified using primers listed in Table S1. The HUB1 DEX-inducible construct and PT4p::HUB1 overexpression construct were made as described previously using Golden Gate cloning (Engler *et al.*, 2014). DEX induction, *Medicago* transformation, spores inoculation and mycorrhizal quantification were performed using the same conditions as described above for *RiNLE1* overexpression.

Isolation of nuclear proteins

Nuclear proteins of *Medicago* roots were isolated as described previously with minor changes (Gendrel *et al.*, 2005). Here, 1 g

of roots was ground to a fine powder in liquid nitrogen and put in 30 ml of extraction buffer 1 (0.4 M sucrose, 10 mM Tris-HCl pH 8, 10 mM MgCl₂, one tablet protease inhibitor cocktail) in a 50-ml tube for 5 min. The solution was filtered through a 70-µm cell strainer into a new 50-ml tube and centrifuged at 3000 *g* at 4°C for 20 min. The pellet was subsequently resuspended in 1 ml of precooled buffer 2 (0.25 M sucrose, 10 mM Tris-HCl pH 8, 10 mM MgCl₂, 1% Triton X-100, one tablet protease inhibitor cocktail) and then transferred into a 1.5-ml microcentrifuge tube and centrifuge at 12 000 *g* at 4°C for 10 min. The resulting pellet was resuspended in 300 µl precooled buffer 3 (1.7 M sucrose, 10 mM Tris-HCl pH 8, 10 mM MgCl₂, 0.15% Triton X-100, one tablet protease inhibitor cocktail). Subsequently, the resuspended mix is layered on top of 300 µl precooled buffer 3 in a new microcentrifuge tube and centrifuged at 15 000 *g* at 4°C for 1 h to pellet nuclei. The nuclear pellet was resuspended in 300 µl RIPA buffer (10 mM Tris-HCl pH 7.5, 150 mM NaCl, 0.1% SDS, 1% Triton X-100, 1% deoxycholate, 0.5 mM EDTA, 20 µM MG132, one tablet protease inhibitor cocktail) by pipetting and vortexing, and then centrifuged at 12 000 *g* at 4°C for 10 min and finally the supernatant containing nuclear proteins was harvested for further analysis.

Western blot

Anti-GFP-HRP and anti-FLAG-HRP antibodies were obtained from Miltenyi Biotec, USA. Ubiquitinated H2B monoclonal antibody (NRO3) was obtained from Medimabs, Canada. Western blots were performed using the Bio-Rad trans-blot turbo system using polyvinylidene difluoride (PVDF) membranes. The blots were blocked using TBS/2% BSA/0.3% Tween-20 and 1 h shaking at room temperature. Here, 1 : 5000 dilutions of the antibodies were used for detection using chemiluminescence and the Clarity Western ECL substrate (Bio-Rad). For detection of H2Bub, a secondary anti-rabbit-HRP antibody was used (1 : 5000 dilution).

Results

RiNLE1 is specifically expressed in arbuscules and translocates to the plant nucleus

Our previous stage-specific transcriptome analysis of the *Rhizophagus irregularis* secretome, identified *c.* 50 putative effector proteins that showed specific expression in arbuscules (Zeng *et al.*, 2018). One of the highest expressed arbuscule-specific effector candidates, RiNLE1 (GenBank: EXX65927.1), was predicted to localise to the nucleus, suggesting that it may translocate to the host cell to exert its function there (Fig. S1a), making it an intriguing candidate effector potentially controlling arbuscule formation.

As a first step to unravel the role of this conserved effector we confirmed the arbuscule-specific expression of *RiNLE1* using RNA *in situ* hybridisation on mycorrhised *Medicago* roots. This showed that *RiNLE1* was indeed specifically expressed in arbuscules, similar to the expression of the arbuscule-containing cell-

specific phosphate transporter 4 (*PT4*; Javot *et al.*, 2007) used as the positive control (Fig. 1a,b). No signal was detected in arbuscules in the negative controls when a RiNLE1 sense probe was used or when probe sets were omitted (Fig. 1c,d).

Next, using a YSST assay, we confirmed that RiNLE1 was secreted as *R. irregularis* currently cannot be stably transformed (Forbes *et al.*, 1998; Helber & Requena, 2008). Therefore, the *RiNLE1* full coding sequence was fused to a yeast invertase (*SUC2*) lacking its endogenous signal peptide and transformed into the *Saccharomyces cerevisiae* Y02321 strain (Lee *et al.*, 2006). Expression of this construct allowed Y02321 to grow on sucrose selection medium, whereas the empty vector control could not (Fig. 2a), indicating the secretion of the RiNLE1-fusion protein.

RiNLE1 contains a nuclear-localisation signal (NLS) at its C-terminus (Fig. S1a). To determine whether RiNLE1 could localise to the plant nucleus in arbuscule-containing cells, we first expressed N-terminal GFP-tagged RiNLE1 (no signal peptide)

by the arbuscule-containing cell-specific *MtPT4* promotor (*PT4p::GFP-RiNLE1*). This showed that GFP-RiNLE1 localised to the nucleus, and especially accumulated in nuclear bodies, including the nucleolus, of arbuscule-containing cells (Fig. 1e–h) similar to its localisation in *Nicotiana benthamiana* leaves (Fig. S1b; Zeng *et al.*, 2018).

Next, we studied whether RiNLE1 could translocate to the host nucleus. We first tried to localise RiNLE1 using specific antibodies. However, despite multiple efforts we were not able to obtain an antibody that was specific enough to reliably detect RiNLE1 *in situ*. Therefore, we used an alternative approach by expressing a GFP-tagged RiNLE1 (no endogenous signal peptide) construct containing a plant signal peptide sequence from *MtBCP1* to target it to the apoplast (Ivanov & Harrison, 2019) under the control of the constitutive *Lotus japonicus Ubiquitin 1* promotor (*LjUB1p::BCPsp-GFP-RiNLE1*) in *Nicotiana* leaves. The *MtBCP1* signal peptide was chosen because the endogenous

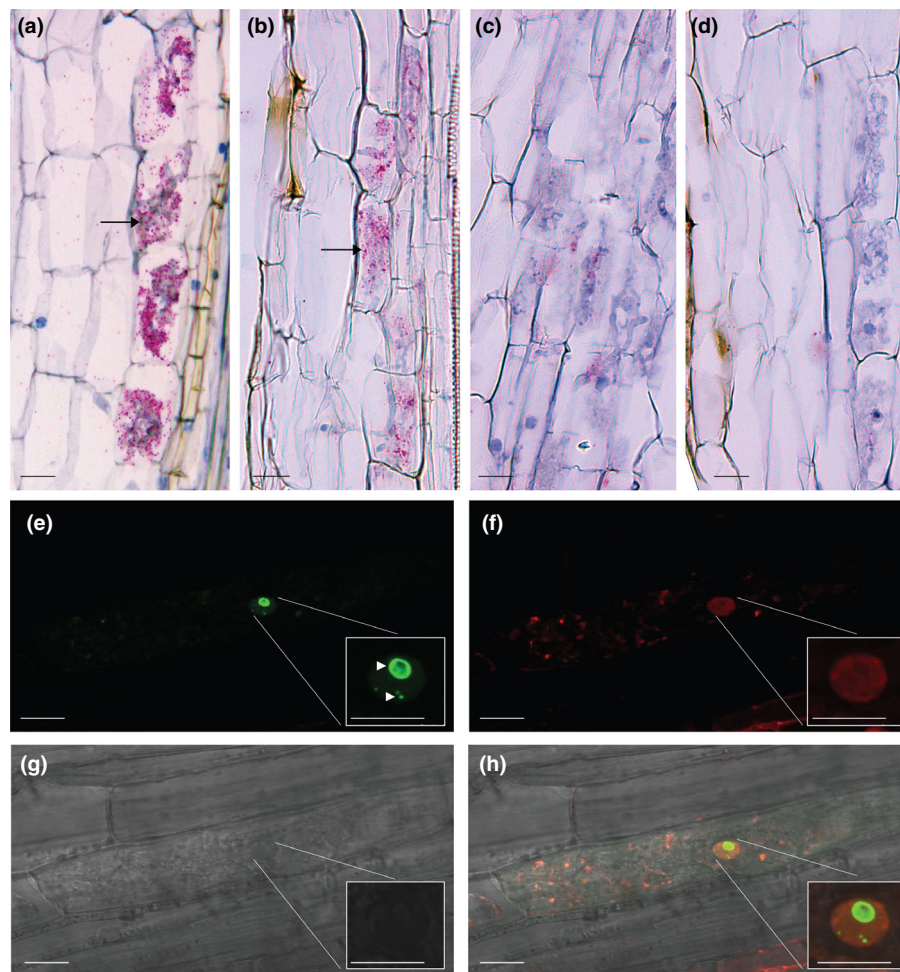


Fig. 1 *RiNLE1* is specifically expressed in arbuscules and localises in the plant nucleus. (a) RNA *in situ* hybridisations of the arbuscule-containing cell-specific *MtPT4* gene in mycorrhised *Medicago truncatula* roots. Arrow indicates *in situ* signal. (b) RNA *in situ* hybridisations of *RiNLE1* in mycorrhised *M. truncatula* roots. Arrow indicates *in situ* signal. (c) Negative control of RNA *in situ* hybridisation in which *RiNLE1* sense probe sets are used. (d) Negative control of RNA *in situ* hybridisation in which probe sets are omitted to reveal the background signal. (a–d) Bars, 25 μ m. (e–h) *PT4p::GFP-RiNLE1 Δ SP* expressed in *M. truncatula* mycorrhizal roots. (e) GFP-RiNLE1 accumulates in the nucleolus and other nuclear bodies of the arbuscule-containing cells, as indicated by arrowheads. (f) Corresponding red fluorescence resulting from co-expression of the DsRed1 protein under the control of the *Arabidopsis thaliana Ubiquitin10* promoter, used as marker for cytoplasm and nucleus. (g) Corresponding bright field image. (h) Corresponding overlay of GFP, DsRed and bright field image. (d–g) Bars, 10 μ m.

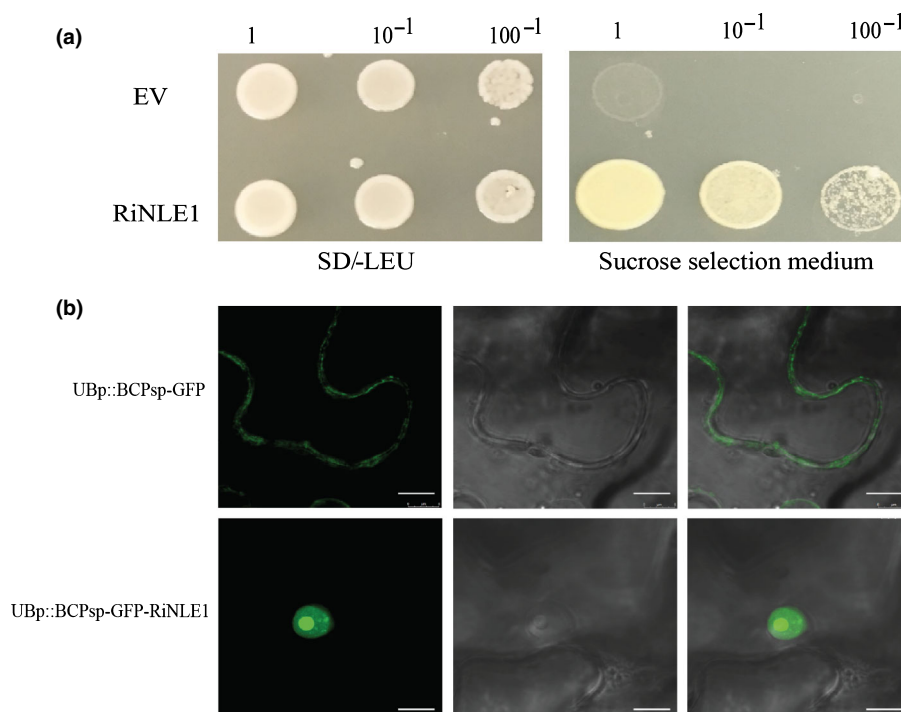


Fig. 2 RiNLE1 is secreted and translocates to the plant nucleus. (a) Yeast signal sequence trap showing that RiNLE1 is a secreted protein. *RiNLE1*, representing a fusion of full-length *RiNLE1* with an invertase, and the empty pYSTO vector (EV) were transformed into *Saccharomyces cerevisiae* Y02321, and grown on SD/–Leu and sucrose selection medium at different dilutions for 3 d at 30°C. (b) RiNLE1 can translocate to the plant nucleus. Expression of *UBp::BCP1sp-GFP* (upper row) and *UBp::MtBCP1sp-GFP-RiNLE1* (lower row), using the signal peptide of Medicago BLUE COPPER PROTEIN 1 (BCP1) to secrete GFP or GFP-tagged RiNLE1 to the apoplast, in *Nicotiana benthamiana* leaves. By contrast with the GFP control, the RiNLE1 fusion protein can be observed inside the plant nucleus indicating that NLE1 can translocate into the plant cell after been secreted to the apoplast. Bars, 10 µm.

signal peptide of RiNLE1 is not well processed in plants, causing an accumulation of recombinant protein in the endoplasmic reticulum (Fig. S1c). *LjUBI::BCPsp-GFP* lacking *RiNLE1* was used as the control. This showed that BCP1sp-GFP-RiNLE1 still accumulated in the nucleolus while the BCPsp-GFP control was only found in the apoplast, suggesting that RiNLE1 can translocate into plant cells even in the absence of the fungus (Fig. 2b). Western blot analyses confirmed the presence of the fusion proteins in *Nicotiana* leaves (Fig. S1d).

Collectively, these results indicated that RiNLE1 is specifically expressed in arbuscules from where it can translocate to the host nucleus.

RiNLE1-like proteins occur in various fungi

To determine whether RiNLE1 homologues can be found in other fungi, we searched for homologues using protein BLAST using NCBI and JGI MycoCosm databases. Numerous hypothetical proteins showing partial homology to part of RiNLE1 were initially identified. To select potential effector homologues among these hits, the following criteria were also applied: (1) the proteins should have a signal peptide predicted using SIGNALP-5.0 (<http://www.cbs.dtu.dk/services/SignalP/>); (1) the proteins should be predicted to be a potential effector based on EFFECTORP 2.0 (<http://effectorp.csiro.au/>); (3) the proteins should have an NLS predicted using LOCALIZER (<http://localizer.csiro.au/>). As a result, 19 homologues of RiNLE1 were identified (Table S3).

These are all hypothetical proteins and lack any known protein domains (Fig. S2a). We could detect the presence of RiNLE1-like effectors containing a signal peptide and a NLS at the C-terminus, in all AM fungal genomes available in NCBI and JGI (Fig. S2a,b). Interestingly, RiNLE1 homologues were also found in ectomycorrhizal fungi *Elaphomyces granulatus* (similarity 37.2%), the water mould parasite fungus *Rozella allomyces* (similarity 43.9%), the green algae parasitic fungus *Powellomyces hirtus* (similarity 41.6%), and the barley powdery mildew fungus *Blumeria graminis* (similarity 37.7%). These results indicated that RiNLE1 homologues exist in a wide range of fungi that intimately interact with plants or that intracellularly colonise other hosts.

Overexpression of RiNLE1 increases AM colonisation

To explore the role of RiNLE1 in mycorrhisation we first applied host-induced gene silencing (HIGS) to knock down its expression (Nowara *et al.*, 2010). However, despite several attempts using two different hairpin constructs, the expression of *RiNLE1* could not be successfully knocked down (data not shown). As an alternative approach we investigated the effect of overexpression of *RiNLE1* on mycorrhizal colonisation. Therefore, *RiNLE1* (without signal peptide) was expressed in Medicago roots under the control of the constitutive *LjUbiquitin1* promoter and mycorrhisation levels were quantified using the intersect method (McGonigle *et al.*, 1990) 3 wk after inoculation. Two

independent repetitions with each of the eight independently transformed roots both showed a significant increase in hyphal abundance compared with the empty vector control, while arbuscule abundance was not significantly changed (Figs 3a, S3). The lack of effect on arbuscule numbers may be because the fungal *RiNLE1* itself is already highly expressed specifically in arbuscule cells. qPCR analyses confirmed overexpression of *RiNLE1* and the phenotype, as the fungal *RiEF1* reference gene was significantly more highly expressed in *UBQp::RiNLE1* roots compared with control roots, while expression of *MtPT4*, a marker for arbuscule abundance, did not significantly change (Fig. 3b). These results indicated that *RiNLE1* plays a positive role in AM colonisation.

RiNLE1 suppresses host defence-related gene expression

As we reasoned that *RiNLE1* exerts its functions inside host nuclei, we explored the influence of *RiNLE1* on plant gene expression. Therefore, we applied a dexamethasone (DEX) inducible promoter system (Borghi, 2010) to induce *RiNLE1* expression (lacking signal peptide) in *Medicago truncatula* roots. As a control we replaced the *RiNLE1* coding sequence using a short non-sense sequence (Dummy3 from the Golden Gate cloning kit; Engler *et al.*, 2014). DEX induction was confirmed 20 h after treatment with 10 μ M DEX by visualising a co-transformed GFP marker that was under the control of the same DEX-inducible *cis*-regulatory element used to drive *RiNLE1* (Fig. S4a,b). qPCR analysis further confirmed the induction of *RiNLE1* (Fig. S4c). Therefore, this time point was chosen to monitor expression changes upon DEX induction using RNA sequencing. Three replicates, representing pools of independently transformed roots, were used for both control and *RiNLE1* samples.

RNA-seq data were analysed using the CLC Genomics workbench 10.0.1 (Qiagen). Read mapping information is summarised in Table S4. PCA of the RNA-seq data showed a clear separation of DEX-*RiNLE1* samples and control DEX-empty

vector (EV) samples in PC2 (27% variance) but not PC1 (49% variance) (Fig. S5a). This indicated that induction of *RiNLE1* impacted gene expression levels, but that there was also a relatively large variation between the different replicate samples. This difference was likely to be caused because different *A. rhizogenes* transformed roots (representing independent transformation events) were analysed for each replicate experiment and the levels of *RiNLE1* expression in the different samples varied; TPM levels for *RiNLE1*: 5215, 1993, 3002 in the three replicates, respectively (bottom row in Table S5). Using a cut-off fold change > 2, and $P < 0.05$, we identified 76 differentially expressed genes (DEGs) in DEX-*RiNLE1* samples relative to DEX-induced control samples (Table S5). Among the identified DEGs, 32 genes were downregulated upon *RiNLE1* induction (Fig. 4a; Table S6).

To determine whether the DEGs would be involved in a common biological process, we performed gene ontology (GO) enrichment analysis (Tian *et al.*, 2017). This revealed a clear enrichment in genes associated with defence or stress-related processes among the 32 downregulated genes (Fig. S5b). By contrast, upregulated genes did not show enrichment in any biological process. Therefore, we specifically focussed on the downregulated genes. The majority of these encoded pathogenesis-related proteins, chitinases or peroxidases, related from plant response to biotic stress (Dodds & Rathjen, 2010) (Fig. 4a; Table S6).

To confirm the RNA-seq data, we selected eight downregulated plant defence-related genes, as well as two strongly upregulated genes, and in an independent experiment quantified their expression levels using qPCR. Except for one gene, all genes showed the expected differential regulation upon *RiNLE1* induction (Fig. 4b). Because *RiNLE1* is specifically expressed in arbuscules, we also analysed whether expression levels of the 32 downregulated genes were lower in arbuscule-containing cells compared with their neighbouring noncolonised cortex cells, based on available cell-specific transcriptome data (Hogekamp & Küster, 2013; Zeng *et al.*, 2018). This experiment showed that the genes, whose expression could be reliably detected, were

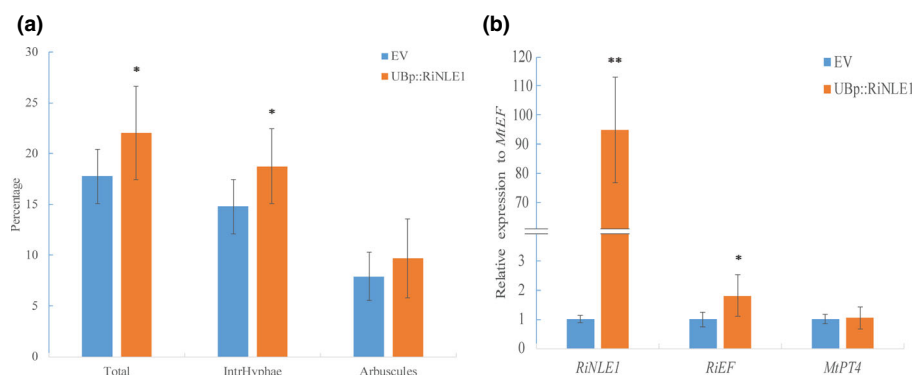


Fig. 3 Overexpression of *RiNLE1* enhances mycorrhizal root colonisation in *Medicago truncatula*. (a) Quantification of the level of mycorrhizal root colonisation in *UBQp::RiNLE1* transgenic roots and empty vector control roots, 3 wk post inoculation. Indicated are the percentage of intraradical hyphae (IntrHyphae), arbuscules and overall level of colonisation (Total). Data are represented as mean \pm SD of eight independently transformed plants per construct. Student's *t*-test. *, $P < 0.05$; (b) qPCR analyses showing increased *RiEF* expression level as the marker for fungal colonisation in *RiNLE1* overexpression samples. No significant difference between EV and *RiNLE1* samples is observed for arbuscular-specific *MtPT4* gene expression. Expression levels were normalised using *MtEF1* as reference. Data are represented as mean \pm SD of eight independently transformed plants per construct. Student's *t*-test. *, $P < 0.05$; **, $P < 0.01$.

© 2021 The Authors
New Phytologist © 2021 New Phytologist Foundation

In subsequent independent Co-IP experiments the interaction of RiNLE1 with the other four proteins (Med36a, H1, Dynamin1, API5; Table S8) enriched in the LC-MS/MS data could not be confirmed (data not shown).

RiNLE1 interferes with H2B mono-ubiquitination

The interaction studies raised the question how RiNLE1 can influence defence gene expression by interacting with H2B? H2B is a core component of nucleosomes and H2B modifications have

been shown to regulate multiple processes from plant development to response to environmental stress (Fleury *et al.*, 2007; Cao *et al.*, 2015; Zhao *et al.*, 2019). Most notably, several studies have reported a link between H2B mono-ubiquitination and plant immune responses (Dhawan *et al.*, 2009; Zou *et al.*, 2014; Zhang *et al.*, 2015). Therefore, we hypothesised that RiNLE1 may influence the mono-ubiquitination of H2B.

To assess the effect of RiNLE1 on H2B ubiquitination (H2Bub), we isolated nuclear proteins from DEX-induced *RiNLE1* overexpression roots and EV control roots. The levels of

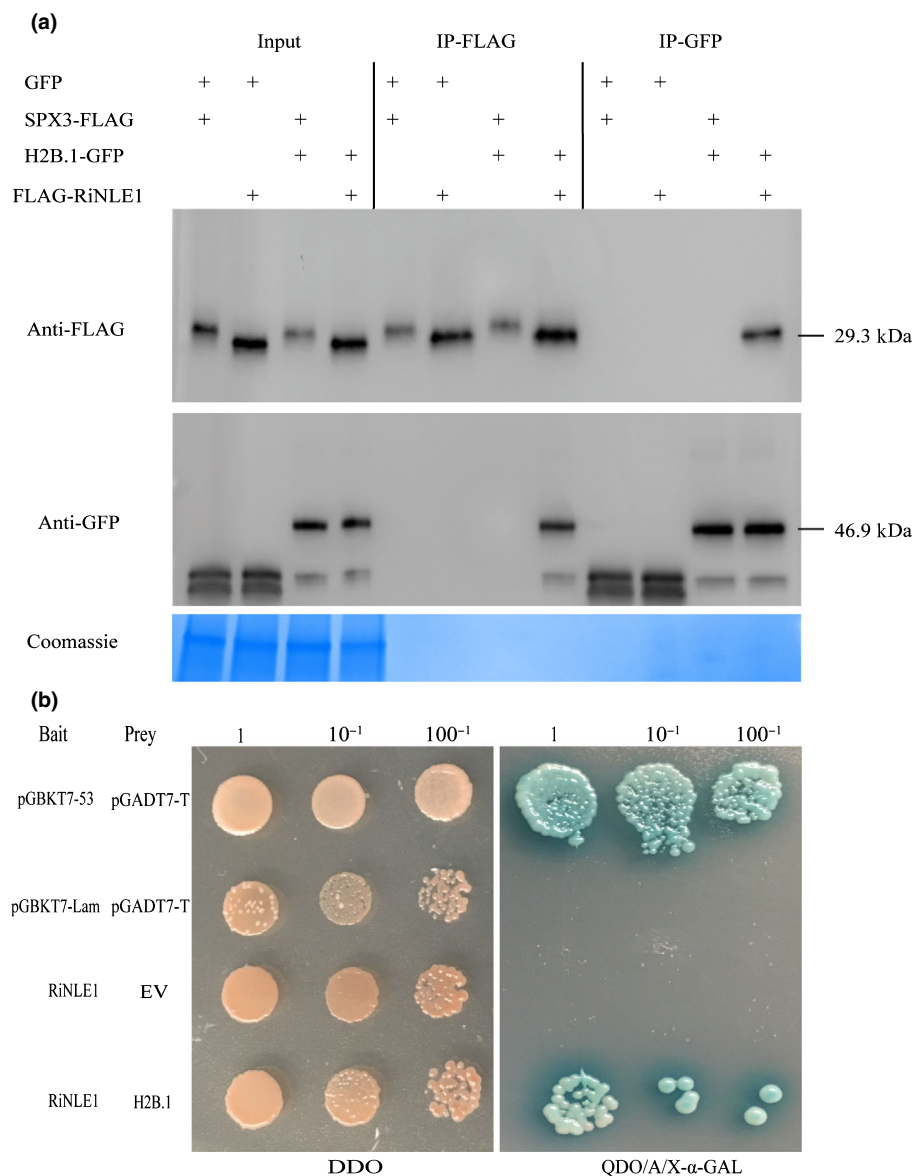


Fig. 5 RiNLE1 interacts with H2B. (a) Co-IP assay in transiently transformed *Nicotiana benthamiana* leaves confirmed the interaction between RiNLE1 and MthH2B.1 (Medtr4g064020). Free GFP and a FLAG-tagged nuclear-localising protein MtSPX3 (Medtr0262s0060) were included as controls. For the input blots, 0.2% input extract was loaded to detect FLAG- and GFP-tagged proteins using anti-FLAG or anti-GFP antibodies, respectively. After co-immunoprecipitation, 20% of the eluate was loaded for detection. Total protein levels were detected using Coomassie brilliant blue staining as the loading control. (b) Y2H assay showing the interaction between RiNLE1 and MthH2B.1, using RiNLE1 as bait (pGBKT7) and H2B.1 as prey (pGADT7). Serial dilutions of overnight mated yeast cultures were plated on selective medium. DDO was used as the control plate to show mating was successful. Selection was carried out on QDO plates containing aureobasidin and LacZ staining as additional selection markers. The positive (pGBKT7_53 + pGADT7_T), negative (pGBKT7_Lam + pGADT7_T), and EV (GBKT7_RiNLE1 + pGADT7) controls are shown.

H2Bub were analysed using western blot and an anti-H2Bub antibody, which detects a conserved mono-ubiquitinated lysine at the C-terminal domain of H2B. The specificity of this antibody has been well tested in *Arabidopsis* (Zou *et al.*, 2014; Chen *et al.*, 2017). As the reference, an antibody against histone 3 was used. Three independent experiments showed that the H2Bub levels were significantly reduced when *RiNLE1* expression was induced (Fig. 6a). Quantification showed a *c.* 40% reduction in H2Bub levels in *RiNLE1*-induced samples (Fig. 6b). This indicates that *RiNLE1* can inhibit H2B mono-ubiquitination in the plant.

H2Bub levels influence defence gene expression and arbuscular mycorrhisation

To establish further that the downregulation of defence-related genes is associated with H2Bub levels, we replaced the H2B predicted mono-ubiquitination site K144 (lysine) to A (alanine), to prevent it from becoming ubiquitinated. We then applied the DEX-inducible system to induce the expression of this modified *H2BK144A* in *Medicago hairy roots* and monitored if its overexpression would affect *RiNLE1*-responsive defence gene expression. DEX-induced wild-type H2B expressing roots were used as control. *H2BK144A* expression was significantly induced 20 h after treatment with 10 μ M DEX (Fig. S7a). Western blot analyses of nuclear protein extracts showed that the *H2BK144A* samples had significantly lower H2Bub levels compared with the EV control (Fig. 7a). Next, we determined the expression level of *RiNLE1*-responsive genes upon suppression of H2Bub levels. Five of them showed significantly lower expression (Fig. 7b), the remainder did not differ. This showed that expression of the genes was suppressed upon inducible overexpression of *H2BK144A* (Fig. 7b). These data indicated that *RiNLE1* can inhibit H2B mono-ubiquitination which in turn hampers the induction of a set of defence-associated genes in arbuscule-containing cells.

To determine whether increased H2Bub levels negatively affected mycorrhisation, we overexpressed the RING E3 ligase H2B monoubiquitination1 (HUB1) enzyme responsible for

H2B ubiquitination (Liu *et al.*, 2007). First, we confirmed that DEX-inducible overexpression of the *Medicago MtHUB1* (Medtr7g046250) orthologue indeed led to higher H2Bub levels in *Medicago roots* (Fig. 7a). Next, we monitored the expression of 10 selected defence genes in response to *MtHUB1* overexpression using qPCR. The expression of four defence genes significantly increased in DEX-induced *MtHUB1* roots compared with EV controls. The expression of two genes showed more complex regulation (Fig. 7e). These data indicated that increased H2Bub levels did affect the expression of *RiNLE1*-responsive defence-related genes.

To study the effect of *MtHUB1* overexpression on mycorrhisation, we expressed *MtHUB1* under the control of the arbuscule-containing cell-specific *MtPT4* promoter in *Medicago roots*. At 3 wk after inoculation the level of mycorrhizal colonisation was scored using the intersect method (McGonigle *et al.*, 1990). Compared with EV control samples, both colonisation level and arbuscule abundance were significantly ($N=8$, $P<0.05$) reduced in *PT4::MtHUB1* overexpression samples. Similar phenotypes were observed in two independent experiments (Fig. 7c). qPCR analyses confirmed the phenotype, using *RiEF* as a marker to represent fungal colonisation level and *MtPT4* as marker for arbuscule abundance (Fig. 7d).

Discussion

Here we show that the arbuscule-specific effector *RiNLE1* can translocate to the host nucleus where it interacts with H2B and can prevent H2B mono-ubiquitination to suppress defence gene activation and promote AM colonisation.

Our results suggest that GFP-tagged *RiNLE1* can translocate to the plant nucleus without the help of other fungal proteins. How effectors in general can translocate into host cells is still an unresolved issue and remains an interesting yet challenging topic to study (Petre & Kamoun, 2014). Irrefutable evidence will require the availability of a specific antibody against *RiNLE1*, which we unfortunately were not able to generate. In the host nucleus, *RiNLE1* accumulated in nuclear bodies, especially the nucleolus (Figs 1e–h, S1b). Nuclear bodies are related to the

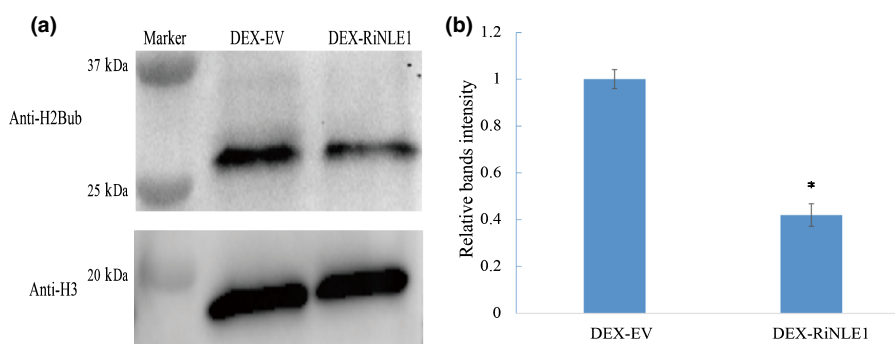


Fig. 6 *RiNLE1* inhibits H2B mono-ubiquitination levels. (a) Western blot analysis of nuclear protein extracts from 20 h DEX-induced EV and *RiNLE1* *Medicago truncatula* roots. Detection was carried out using anti-H2Bub (upper panel) or anti-H3 antibody (lower panel). The expected sizes of H2Bub and H3 are 28 kDa and 17 kDa, respectively. Similar results were obtained in three independent experiments. (b) Quantification of the relative band intensities using IMAGEJ software based on the three independent experiments, including the one shown in (a), normalised to H3 levels. Error bars indicate SD from the three replicates. Student's *t*-test was used. *, $P<0.05$.

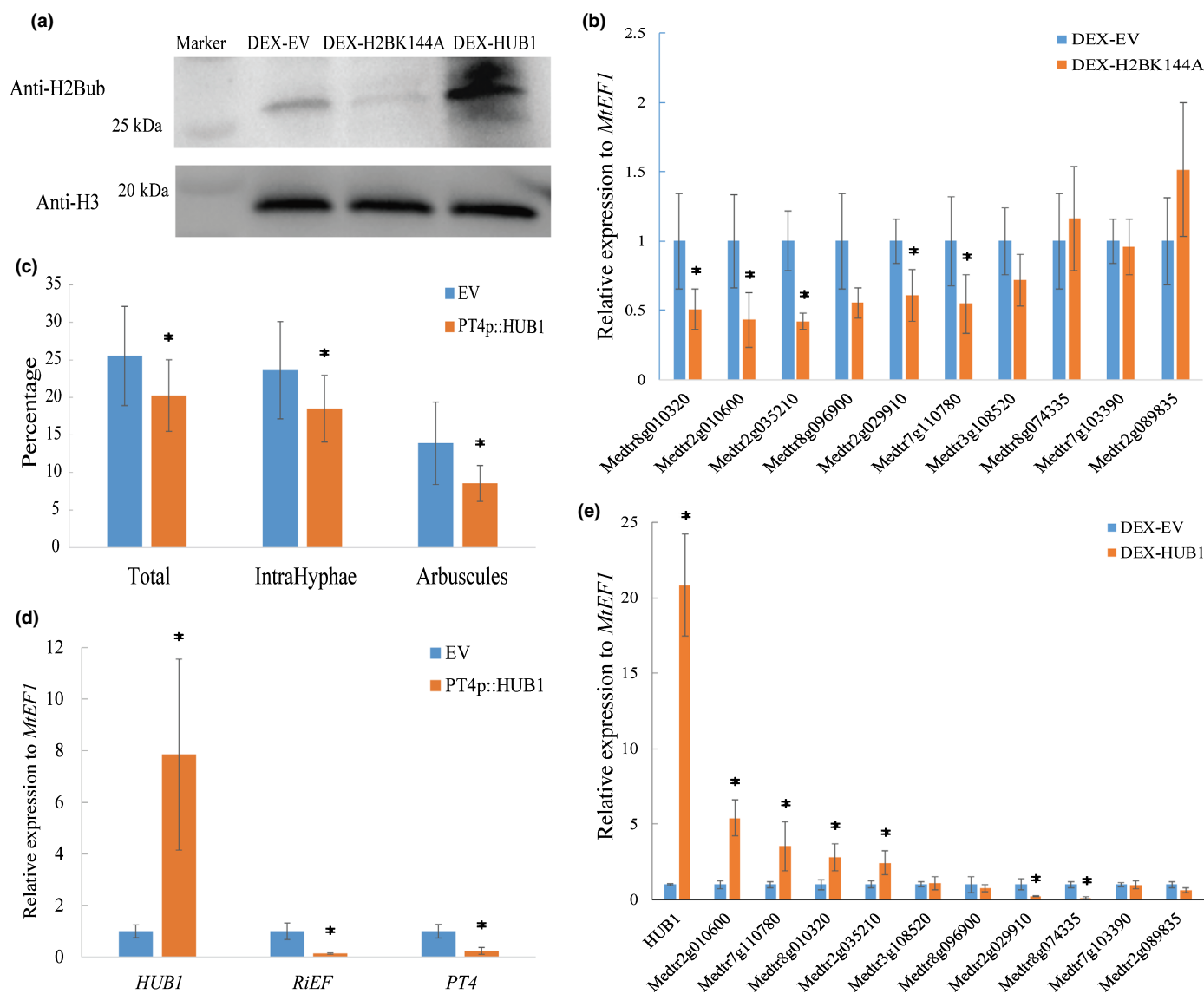


Fig. 7 H2Bub levels influence defence gene expression and arbuscular mycorrhisation. (a) Western blot analysis of nuclear protein extracts from 20 h DEX-induced EV, *Mth2BK144A* and *MthHUB1* expressing Medicago roots. Detection using anti-H2Bub (upper panel) and anti-H3 antibody (lower panel). (b) qPCR analysis of selected defence-related genes in DEX-induced *H2BK144A* roots compared with EV induced roots. *MtEF1* was used as the reference gene. Medtr8g010320, Defensin related; Medtr2g010600, Catabolite activator protein (CAP); Medtr2g035210, ABA-responsive protein; Medtr8g096900, pathogenesis-related thaumatin family protein; Medtr2g029910, peroxidase family protein; Medtr7g110780, Chitinase, Medtr3g108520, gibberellin 2-beta-dioxygenase; Medtr8g074335, Chitinase (Class Ib)/Hevein; Medtr7g103390, Myb/SANT-like DNA-binding domain protein; Medtr2g089835, wound-responsive family protein. Error bars indicate SD from three replicates. (c) Quantification of mycorrhisation in eight independently transformed *M. truncatula* roots expressing *PT4p::MthHUB1* and eight EV transformed roots as control at 3 wk post inoculation with *Rhizophagus irregularis* using the intersect method. Student's *t*-test was used. **P* < 0.05. Data are represented as mean \pm SD. (d) qPCR analyses of *MthHUB1*, *RiEF* and *MthPT4* in *PT4p::MthHUB1* expressing and EV. *MtEF1* was used as reference. Data are represented as mean \pm SD of eight biological replicates. Student's *t*-test. **P* < 0.05. (e) qRT-PCR analysis of defence-related gene expression from DEX-induced *MthHUB1* samples compared with DEX-induced EV samples. *MtEF1* was used as reference. Data are represented as mean \pm SD of three biological replicates. Student's *t*-test was used. **P* < 0.05.

formation of ribonucleoprotein complexes, processing of RNA and epigenetic regulation of gene expression (Shaw & Brown, 2004; Mao *et al.*, 2011). Although we could rule out that RiNLE1 exerts its function specifically in these nuclear bodies, the observed accumulation could also be an artefact of overexpression. As for GFP-RiNLE1, H2B-GFP also accumulated in the nucleolus when it was expressed in *Nicotiana* leaves under the control of a strong constitutive promoter (Fig. S7b,c). Similar observations have been made for GFP-tagged H2B in other

systems. Musinova *et al.* (2011) identified a nucleolar localisation/retention signal (NoRS) in the H2B protein, enabling it to exchange between the nucleolus and nucleoplasm in human cell lines. A potential NoRS enriched with basic amino acids can also be found in RiNLE1 (KKKGKKGKPKRKH), which may cause nonspecific retention in the nucleolus, especially when expressed under a strong promoter (Musinova *et al.*, 2011).

We observed a downregulation of a subset of defence-related genes upon overexpression of both *RiNLE1* and a non-

monoubiquitinated H2B form in *Medicago* roots. Arbuscule abundance was not affected upon *RiNLE1* overexpression, which is likely to be due to the high endogenous expression levels of *RiNLE1* specifically in the arbuscules. This factor may limit the effect of additional expression of *RiNLE1* in these cells by the *LjUbiquitin* promoter. Conversely, overexpression of *MtHUB1* caused increased H2Bub levels and increased expression of *RiNLE1*-regulated defence-related genes, which correlated with lower AM colonisation levels. Similar observations linking H2B mono-ubiquitination to defence have been reported in relation to pathogenic interactions. For example, in *Arabidopsis* H2B mono-ubiquitination has been shown to be required for transcriptional activation of resistance (R) genes *SNC1* and *RPP4*, involved in the resistance to necrotrophic fungal pathogens (Zou *et al.*, 2014). Overexpression of *HUB1* led to resistance, whereas *hub1* loss-of-function mutants showed increased susceptibility to these fungi (Dhawan *et al.*, 2009; Zou *et al.*, 2014). Increased H2Bub levels also caused increased resistance against *Botrytis cinerea* by balancing the SA- and JA/ET-mediated signalling pathways in tomato (Zhang *et al.*, 2015). How H2B mono-ubiquitination or *RiNLE1* affects specific genes is currently not known. The binding of *RiNLE1* to H2B may obstruct the accessibility of *HUB1* to mono-ubiquitinate H2B.

H2Bub has also been shown to be involved in histone crosstalk, mediating for example the methylation of H3 (Sun & Allis, 2002; Zhao *et al.*, 2019). *Arabidopsis hub1* and *hub2* mutants show reduced H3 methylation levels at several gene loci that regulate plant flowering time, indicating that H2Bub can enhance H3 methylation (Cao *et al.*, 2008). Interestingly, in *hub1* mutants, the H3K4me2 levels were also reduced at the *R* gene *SNC1* locus, suggesting that H2Bub-mediated H3 methylation also regulates defence responses (Lee *et al.*, 2016). Therefore it would be interesting to follow-up whether *RiNLE1* similarly affects other histone modifications in arbuscule-containing cells and whether it affects other genes that may be important for the symbiosis. Furthermore, beside mono-ubiquitination various other post-translation H2B modifications have been reported to affect gene expression that could be influenced by *RiNLE1*, but most of these are not yet well studied in plants.

To our knowledge this is the first example of a fungal effector directly targeting a core nucleosome histone protein, H2B, to control epigenetic modifications. So far, pathogenic effectors that affect histone modifications have been found to operate through their interaction with histone modifying enzymes (Ransom & Walton, 1997; Walley *et al.*, 2008; Kong *et al.*, 2017; Li *et al.*, 2018; Ramirez-Prado *et al.*, 2018). Whether *RiNLE1* can also affect other post-translational H2B modifications remains to be studied. The other known example of a pathogen directly targeting a histone protein is the 6b oncoprotein encoded in the T-DNA of *Agrobacterium tumefaciens*. This protein was shown to act as a histone chaperone, interacting specifically with histone 3 to control cell divisions (Terakura *et al.*, 2007).

Interestingly, we found that, in addition to being conserved in AM fungi, *RiNLE1*-like effectors occurred in a variety of (biotrophic) pathogenic and mutualistic fungal species. This suggests that H2B may be a common target for such fungal effector

proteins. The occurrence of a *RiNLE1*-type effector in the water mould parasitic fungus *Rozella allomyces* (Fig. S2; Table S3), which intracellularly colonises *Allomyces* species, suggests that *NLE1*-type effectors may even reflect a broader fungal strategy to colonise other hosts (James *et al.*, 2013; Gan *et al.*, 2019).

It has become clear that interference with the chromatin organisation of plants is a common strategy used by pathogenic microbes to subvert the host immune system (Ramirez-Prado *et al.*, 2018). Our finding that also mutualistic AM fungi use effector proteins to modify the plants epigenome further supports the idea that pathogenic and mutualistic microbes use comparable strategies to interact with their plant hosts. We envision that more studies on the epigenomic reprogramming that occurs during AM symbiosis will be a promising avenue to understand this fundamental symbiosis in plants.




Acknowledgements

The authors declare no conflict of interest. PW is supported by the China Scholarship Council (CSC) grant: 201606310038. *Agrobacterium* strains containing expression constructs for *SlCf-4* and *CfAVR-4* were kindly provided by Matthieu Joosten (Laboratory of Phytopathology, Wageningen University & Research).

Author contributions

PW and EL conceived and designed experiments. PW, HJ and HD performed experiments and/or data analyses. SB performed LC-MS/MS. OK performed RNA *in situ*. PW, TB and EL wrote the manuscript.

ORCID

Ton Bisseling  <https://orcid.org/0000-0001-5494-8786>
Erik Limpens  <https://orcid.org/0000-0002-9668-4085>
Peng Wang  <https://orcid.org/0000-0002-1541-2396>

References

- Bielow C, Mastrobuoni G, Kempa S. 2016. Proteomics quality control: quality control software for MaxQuant results. *Journal of Proteome Research* 15: 777–787.
- Borghi L. 2010. *Inducible gene expression systems for plants*. Hertfordshire, UK: Humana Press.
- Cao H, Li X, Wang Z, Ding M, Sun Y, Dong F, Chen F, Liu L, Doughty J, Li Y *et al.* 2015. Histone H2B monoubiquitination mediated by HISTONE MONOUBIQUITINATION1 and HISTONE MONOUBIQUITINATION2 is involved in anther development by regulating tapetum degradation-related genes in rice. *Plant Physiology* 168: 1389–1405.
- Cao Y, Dai Y, Cui S, Ma L. 2008. Histone H2B monoubiquitination in the chromatin of Flowering Locus C regulates flowering time in *Arabidopsis*. *Plant Cell* 20: 2586–2602.
- Chen S, Jing Y, Kang X, Yang L, Wang DL, Zhang W, Zhang L, Chen P, Chang JF, Yang XM *et al.* 2017. Histone H2B monoubiquitination is a critical epigenetic switch for the regulation of autophagy. *Nucleic Acids Research* 45: 1144–1158.
- Cox J, Hein MY, Luber CA, Paron I, Nagaraj N, Mann M. 2014. Accurate proteome-wide label-free quantification by delayed normalization and maximal

- peptide ratio extraction, termed MaxLFQ. *Molecular and Cellular Proteomics* 13: 2513–2526.
- Dhawan R, Luo H, Foerster AM, Abuqamar S, Du HN, Briggs SD, Scheid OM, Mengiste T. 2009. HISTONE MONOUBIQUITINATION1 interacts with a subunit of the mediator complex and regulates defense against necrotrophic fungal pathogens in Arabidopsis. *Plant Cell* 21: 1000–1019.
- Dodds PN, Rathjen JP. 2010. Plant immunity: towards an integrated view of plant-pathogen interactions. *Nature Reviews Genetics* 11: 539–548.
- Engler C, Youles M, Gruetzner R, Ehnert TM, Werner S, Jones JDG, Patron NJ, Marillonnet S. 2014. A Golden Gate modular cloning toolbox for plants. *ACS Synthetic Biology* 3: 839–843.
- Fleury D, Himanen K, Cnops G, Nelissen H, Boccardi TM, Maere S, Beemster GTS, Neyt P, Anami S, Robles P *et al.* 2007. The *Arabidopsis thaliana* homolog of yeast BRE1 has a function in cell cycle regulation during early leaf and root growth. *Plant Cell* 19: 417–432.
- Forbes PJ, Millam S, Hooker JE, Harrier LA. 1998. Transformation of the arbuscular mycorrhiza *Gigaspora rosea* by particle bombardment. *Mycological Research* 102: 497–501.
- Gan P, Tsushima A, Hiroyama R, Narusaka M, Takano Y, Narusaka Y, Kawaradani M, Damm U, Shirasu K. 2019. *Colletotrichum shioi* sp. nov., an anthracnose pathogen of *Perilla frutescens* in Japan: molecular phylogenetic, morphological and genomic evidence. *Scientific Reports* 9: 13349.
- García-Garrido JM, Ocampo JA. 2002. Regulation of the plant defence response in arbuscular mycorrhizal symbiosis. *Journal of Experimental Botany* 53: 1377–1386.
- Gendrel AV, Lippman Z, Martienssen R, Colot V. 2005. Profiling histone modification patterns in plants using genomic tiling microarrays. *Nature Methods* 2: 213–218.
- Gutjahr C, Parniske M. 2013. Cell and developmental biology of arbuscular mycorrhiza symbiosis. *Annual Review of Cell and Developmental Biology* 29: 593–617.
- Helber N, Requena N. 2008. Expression of the fluorescence markers DsRed and GFP fused to a nuclear localization signal in the arbuscular mycorrhizal fungus *Glomus intraradices*. *New Phytologist* 177: 537–548.
- Hogekamp C, Küster H. 2013. A roadmap of cell-type specific gene expression during sequential stages of the arbuscular mycorrhiza symbiosis. *BMC Genomics* 14: 306.
- Ivanov S, Harrison MJ. 2019. Accumulation of phosphoinositides in distinct regions of the periarbuscular membrane. *New Phytologist* 221: 2213–2227.
- James TY, Pelin A, Bonen L, Ahrendt S, Sain D, Corradi N, Stajich JE. 2013. Shared signatures of parasitism and phylogenomics unite cryptomycota and microsporidia. *Current Biology* 23: 1548–1553.
- Javot B, Penmetza RV, Terzaghi N, Cook DR, Harrison MJ. 2007. A *Medicago truncatula* phosphate transporter indispensable for the arbuscular mycorrhizal symbiosis. *Proceedings of the National Academy of Sciences, USA* 104: 1720–1725.
- Jenner RG, Young RA. 2005. Insights into host responses against pathogens from transcriptional profiling. *Nature Reviews Microbiology* 3: 281–294.
- Kamel L, Tang N, Malbreil M, San Clemente H, Le Marquer M, Roux C, ditFrey NF. 2017. The comparison of expressed candidate secreted proteins from two arbuscular mycorrhizal fungi unravels common and specific molecular tools to invade different host plants. *Frontiers in Plant Science* 8: 1–18.
- Kloppholz S, Kuhn H, Requena N. 2011. A secreted fungal effector of *Glomus intraradices* promotes symbiotic biotrophy. *Current Biology* 21: 1204–1209.
- Kong L, Qiu X, Kang J, Wang Y, Chen H, Huang J, Qiu M, Zhao Y, Kong G, Ma Z *et al.* 2017. A phytophthora effector manipulates host histone acetylation and reprograms defense gene expression to promote infection. *Current Biology* 27: 981–991.
- Kulikova O, Franken C, Bisseling T. 2018. In situ hybridization method for localization of mRNA molecules in *Medicago* tissue sections. In: Cañas LA, Beltrán JP, eds. *Functional genomics in Medicago truncatula: Methods and protocols*. New York, NY: Springer, New York, 145–159.
- Lee S, Fu F, Xu S, Lee SY, Yun DJ, Mengiste T. 2016. Global regulation of plant immunity by histone lysine methyl transferases. *Plant Cell* 28: 1640–1661.
- Lee S-J, Kelley BS, Damasceno CMB, John BSt, Kim B-S, Kim B-D, Rose JKC. 2006. A functional screen to characterize the secretomes of eukaryotic pathogens and their hosts *in planta*. *Molecular Plant–Microbe Interactions* 19: 1368–1377.
- Li H, Wang H, Jing M, Zhu J, Guo B, Wang Y, Lin Y, Chen H, Kong L, Ma Z *et al.* 2018. A Phytophthora effector recruits a host cytoplasmic transacetylase into nuclear speckles to enhance plant susceptibility. *eLife* 7: 1–23.
- Liebrand TWH, van den Berg GCM, Zhao Z, Smit P, Cordewener JHG, America AHP, Sklenar J, Jones AME, Tameling WIL, Robatzek S *et al.* 2013. Receptor-like kinase SOBIR1/EVR interacts with receptor-like proteins in plant immunity against fungal infection. *Proceedings of the National Academy of Sciences, USA* 110: 13228.
- Limpens E, Ramos J, Franken C, Raz V, Compaan B, Franssen H, Bisseling T, Geurts R. 2004. RNA interference in *Agrobacterium rhizogenes*-transformed roots of Arabidopsis and *Medicago truncatula*. *Journal of Experimental Botany* 55: 983–992.
- Lin K, Limpens E, Zhang Z, Ivanov S, Saunders DGO, Mu D, Pang E, Cao H, Cha H, Lin T *et al.* 2014. Single nucleus genome sequencing reveals high similarity among nuclei of an Endomycorrhizal fungus. *PLoS Genetics* 10: e1004078.
- Liu Y, Koornneef M, Soppe WJJ. 2007. The absence of histone H2B monoubiquitination in the Arabidopsis hub1 (rdo4) mutant reveals a role for chromatin remodeling in seed dormancy. *Plant Cell* 19: 433–444.
- Lo Presti L, Lanver D, Schweizer G, Tanaka S, Liang L, Tollot M, Zuccaro A, Reissmann S, Kahmann R. 2015. Fungal effectors and plant susceptibility. *Annual Review of Plant Biology* 66: 513–545.
- Lu J, Boeren S, de Vries SC, van Valenberg HJF, Vervoort J, Hettinga K. 2011. Filter-aided sample preparation with dimethyl labeling to identify and quantify milk fat globule membrane proteins. *Journal of Proteomics* 75: 34–43.
- Ma L, Lukasik E, Gawehns F, Takken FLW. 2012. The use of agroinfiltration for transient expression of plant resistance and fungal effector proteins in *Nicotiana benthamiana* leaves. In: Bolton MD, Thomma BPHJ, eds. *Plant fungal pathogens: Methods and protocols*. Totowa, NJ, USA: Humana Press, 61–74.
- Mao YS, Zhang B, Spector DL. 2011. Biogenesis and function of nuclear bodies. *Trends in Genetics* 27: 295–306.
- McGonigle TP, Miller MH, Evans DG, Fairchild GL, Swan JA. 1990. A new method which gives an objective measure of colonization of roots by vesicular-arbuscular mycorrhizal fungi. *New Phytologist* 115: 495–501.
- Musinova YR, Lisitsyna OM, Golyshev SA, Tuzhikov AI, Polyakov VY, Sheval EV. 2011. Nucleolar localization/retention signal is responsible for transient accumulation of histone H2B in the nucleolus through electrostatic interactions. *Biochimica et Biophysica Acta – Molecular Cell Research* 1813: 27–38.
- Nowara D, Schweizer P, Gay A, Lacomme C, Shaw J, Ridout C, Douchkov D, Hensel G, Kümlehn J. 2010. HIGS: Host-induced gene silencing in the obligate biotrophic fungal pathogen *Blumeria graminis*. *Plant Cell* 22: 3130–3141.
- Petre B, Kamoun S. 2014. How do filamentous pathogens deliver effector proteins into plant cells? *PLoS Biology* 12: e1001801.
- Ramirez-Prado JS, Abulfaraj AA, Rayapuram N, Benhamed M, Hirt H. 2018. Plant immunity: from signaling to epigenetic control of defense. *Trends in Plant Science* 23: 833–844.
- Ransom RF, Walton JD. 1997. Histone hyperacetylation in maize in response to treatment with HC-toxin or infection by the filamentous fungus *Cochliobolus carbonum*. *Plant Physiology* 115: 1021–1027.
- Shaw PJ, Brown JW. 2004. Plant nuclear bodies. *Current Opinion in Plant Biology* 7: 614–620.
- Smaczniak C, Li N, Boeren S, America T, Van Dongen W, Goerdal SS, De Vries S, Angenent GC, Kaufmann K. 2012. Proteomics-based identification of low-abundance signaling and regulatory protein complexes in native plant tissues. *Nature Protocols* 7: 2144–2158.
- Smith S, Read D. 2008. *Mycorrhizal symbiosis*. Cambridge, UK: Academic Press.
- Sun ZW, Allis CD. 2002. Ubiquitination of histone H2B regulates H3 methylation and gene silencing in yeast. *Nature* 418: 104–108.
- Terakura S, Ueno Y, Tagami H, Kitakura S, Machida C, Wabiko H, Aiba H, Otten L, Tsukagoshi H, Nakamura K *et al.* 2007. An oncoprotein from the plant pathogen *Agrobacterium* has histone chaperone-like activity. *Plant Cell* 19: 2855–2865.

- Tian T, Liu Y, Yan H, You Q, Yi X, Du Z, Xu W, Su Z. 2017. AgriGO v2.0: A GO analysis toolkit for the agricultural community, 2017 update. *Nucleic Acids Research* 45: W122–W129.
- Tisserant E, Malbreil M, Kuo A, Kohler A, Symeonidi A, Balestrini R, Charron P, Duensing N, Frei Dit Frey N, Gianinazzi-Pearson V *et al.* 2013. Genome of an arbuscular mycorrhizal fungus provides insight into the oldest plant symbiosis. *Proceedings of the National Academy of Sciences, USA* 110: 20117–20122.
- Volpin H, Elkind Y, Okon Y, Kapulnik Y. 1994. A vesicular arbuscular mycorrhizal fungus (*Glomus intraradix*) induces a defense response in alfalfa roots. *Plant Physiology* 104: 683–689.
- Voß S, Betz R, Heidt S, Corradi N, Requena N. 2018. RiCRN1, a crinkler effector from the arbuscular mycorrhizal fungus *Rhizophagus irregularis*, functions in arbuscule development. *Frontiers in Microbiology* 9: 1–18.
- Walley JW, Rowe HC, Xiao Y, Chehab EW, Kliebenstein DJ, Wagner D, Dehesh K. 2008. The chromatin remodeler SPLAYED regulates specific stress signaling pathways. *PLoS Pathogens* 4: e1000237.
- Wawra S, Fesel P, Widmer H, Timm M, Seibel J, Leson L, Kessler L, Nostadt R, Hilbert M, Langen G *et al.* 2016. The fungal-specific β -glucan-binding lectin FGB1 alters cell-wall composition and suppresses glucan-triggered immunity in plants. *Nature Communications* 7: 13188.
- Wendrich JR, Boeren S, Möller BK, Weijers D, De Rybe LB. 2017. *In vivo* identification of plant protein complexes using IP-MS/MS. In: Kleine-Vehn J, Sauer M, eds. *Methods in molecular biology*. New York, NY, USA: Springer, New York, 147–158.
- Young ND, Debellé F, Oldroyd GED, Geurts R, Cannon SB, Udvardi MK, Bénédict VA, Mayer KFX, Gouzy J, Schoof H. 2011. The *Medicago* genome provides insight into the evolution of rhizobial symbioses. *Nature* 480: 520–524.
- Zeng T, Holmer R, Hontelez J, te Lintel-Hekkert B, Marufu L, de Zeeuw T, Wu F, Schijlen E, Bisseling T, Limpens E. 2018. Host- and stage-dependent secretome of the arbuscular mycorrhizal fungus *Rhizophagus irregularis*. *The Plant Journal* 94: 411–425.
- Zeng T, Rodriguez-Moreno L, Mansurkhodzhev A, Wang P, van den Berg W, Gascoli V, Cottaz S, Fort S, Thomma BPHJ, Bono JJ *et al.* 2020. A lysin motif effector subverts chitin-triggered immunity to facilitate arbuscular mycorrhizal symbiosis. *New Phytologist* 225: 448–460.
- Zhang Y, Li D, Zhang H, Hong Y, Huang L, Liu S, Li X, Ouyang Z, Song F. 2015. Tomato histone H2B monoubiquitination enzymes SIHUB1 and SIHUB2 contribute to disease resistance against *Botrytis cinerea* through modulating the balance between SA- and JA/ET-mediated signaling pathways. *BMC Plant Biology* 15: 252.
- Zhao W, Neyt P, Van Lijsebettens M, Shen WH, Berr A. 2019. Interactive and noninteractive roles of histone H2B monoubiquitination and H3K36 methylation in the regulation of active gene transcription and control of plant growth and development. *New Phytologist* 221: 1101–1116.
- Zou B, Yang DL, Shi Z, Dong H, Hua J. 2014. Monoubiquitination of histone 2B at the disease resistance gene locus regulates its expression and impacts immune responses in Arabidopsis. *Plant Physiology* 165: 309–318.

Supporting Information

Additional Supporting Information may be found online in the Supporting Information section at the end of the article.

Fig. S1 RiNLE1 information.

Fig. S2 RiNLE1-like proteins occur in a variety of fungal species.

Fig. S3 Overexpression of RiNLE1 enhances AMF colonisation.

Fig. S4 Dexamethasone induction of *RiNLE1* expression.

Fig. S5 RNA-seq analysis of *RiNLE1*-induced *Medicago truncatula* transgenic roots.

Fig. S6 Anti-FLAG western blot confirming the expression of FLAG-RiNLE1 fusion protein in *Medicago truncatula* roots and anti-FLAG immunoprecipitation.

Fig. S7 Dexamethasone induction of modified *H2B* expression and H2B localisation in *Nicotiana benthamiana* leaves.

Table S1 List of primers used in this work.

Table S2 Constructs made using the Golden Gate system.

Table S3 RiNLE1 homologues from fungal species based on protein BLAST using NCBI and JGI MycoCosm databases.

Table S4 RNA-seq data mapping statistics generated using CLC Genomics workbench 10.0.1 (Qiagen).

Table S5 Expression browser of DEX-EV and DEX-RiNLE1 RNA-seq data.

Table S6 RNA-seq expression data of genes downregulated upon RiNLE1 induction.

Table S7 Expression of RiNLE1-regulated defence-related genes in arbuscules (ARB) and neighbouring noncolonised cortex cells (HYP).

Table S8 LC-MS/MS identified peptide intensity information for FLAG-RiNLE1 co-immunoprecipitation.

Please note: Wiley Blackwell are not responsible for the content or functionality of any Supporting Information supplied by the authors. Any queries (other than for missing material) should be directed to the *New Phytologist* Central Office.